

**UCC Library and UCC researchers have made this item openly available.
Please [let us know](#) how this has helped you. Thanks!**

Title	The sound of salts by Broadband Acoustic Resonance Dissolution Spectroscopy
Author(s)	van Ruth, Saskia; Dekker, Pieter; Brouwer, Erwin; Rozijn, Maikel; Erasmus, Sara; Fitzpatrick, Dara
Publication date	2018-09-24
Original citation	van Ruth, S., Dekker, P., Brouwer, E., Rozijn, M., Erasmus, S. and Fitzpatrick, D., 2019. The sound of salts by Broadband Acoustic Resonance Dissolution Spectroscopy. Food Research International, 116, (12pp). DOI:10.1016/j.foodres.2018.09.044
Type of publication	Article (peer-reviewed)
Link to publisher's version	http://www.sciencedirect.com/science/article/pii/S0963996918307634 http://dx.doi.org/10.1016/j.foodres.2018.09.044 Access to the full text of the published version may require a subscription.
Rights	© 2018 The Author(s). Published by Elsevier Ltd https://creativecommons.org/licenses/by-nc-nd/4.0/
Item downloaded from	http://hdl.handle.net/10468/8642

Downloaded on 2021-11-27T10:05:51Z



The sound of salts by Broadband Acoustic Resonance Dissolution Spectroscopy



Saskia van Ruth^{a,b,c,*}, Pieter Dekker^a, Erwin Brouwer^a, Maikel Rozijn^a, Sara Erasmus^a, Dara Fitzpatrick^b

^a Wageningen University and Research, P.O. Box 230, 6700 AE Wageningen, The Netherlands

^b University College Cork, Cork, Ireland

^c Queen's University Belfast, Northern Ireland, UK

ARTICLE INFO

Keywords:

Authenticity
BARDS
Food identity
Provenance
Resonance
Sound spectroscopy

ABSTRACT

Salts are available in different grades and in a wide price range. Some contain more impurities than others, while some have special culinary traits that determine their identity. Acoustic profiling, which is based on the 'hot chocolate effect', may provide an interesting strategy to characterise salts of various origins to underpin their identity. In this study, the link between the identity of 60 food grade and technical salts and their acoustic properties was examined by Broad Acoustic Resonance Dissolution Spectroscopy. In particular, the influence of the composition of the salts and the impact of the salts' particle size distributions on their acoustic profiles were examined. Sodium and potassium contents were measured by flame photometry and the salts' particle size distributions by laser light diffraction. Reference salts (NaCl, KCl, MgCl₂) and mixtures thereof were analysed for comparison, as well as intact and ground versions of the salt samples. The results show that both the composition and morphology of the salt crystals determine the down-slope of the resonance frequency, which is caused by the rate of release of entrained and dissolved gas. Coarse salts with high levels of non-NaCl constituents showed a rapid decline in sound frequency, which corresponds to a high gas release rate. On the other hand fine salts composed of pure NaCl revealed a slower change in sound frequency and thus lower gas release rates. The frequency minimums were however not affected by the salts' compositions nor particle size distributions. It is primarily the particle size distribution that affects the rate at which gas is released, and thus the change in sound frequency. Only when the particles are more similar in size, the composition also starts playing a role. Since both particle size distribution and composition is unique for each salt, the various salts show distinct acoustic profiles. Evidently, the current study shows that 'listening' to the sound of salts reveals interesting information about their identity and origin.

1. Introduction

Salt is the common name for the chemical compound sodium chloride (NaCl). For several millennia salt has been known as a valuable seasoning and it has been used as a preservative for centuries (Aquilano, Otálora, Pastero, and García-Ruiz (2016). Even the word 'salary' originates from the Latin word for salt (Etymonline, 2017). All salt came from the sea at some point, and may currently be present either in solution or in crystallized form. The open ocean contains about 35 g of solids per liter and comprises six main components, the cations Na⁺, Mg⁺⁺, Ca⁺⁺, K⁺, and the anions Cl⁻ and SO₄⁻ (Braitsch, 1971). In addition to these main components, some other compounds

may be present at lower concentrations: over 30 minerals have been determined in salt deposits, among which are sulphates, silicates, halides, oxides and hydroxides, sulphides and others (Fernández-López, Faz Cano, Arocena, & Alcolea, 2014).

Salt is processed from salt mines (i.e. rock salt), or by the evaporation of sea/mineral-rich spring water. Rock salt is simply crystallized salt, also known as halite, and is the result of evaporation of ancient oceans. Large deposits of rock salt are found in North America, China, and central and eastern Europe. Inland lakes such as the Dead Sea in the middle East and the Great Salt Lake in the USA are also locations where this kind of deposits are formed, also today. These salts are either mined directly or are extracted in solution by pumping water

* Corresponding author at: Wageningen University and Research, P.O. Box 230, 6700 AE Wageningen, The Netherlands.

E-mail addresses: saskia.vanruth@wur.nl, saskia.ruth@qub.ac.uk (S. van Ruth), Pieter.dekker@wur.nl (P. Dekker), Erwin.brouwer@wur.nl (E. Brouwer), Maikel.rozijn@wur.nl (M. Rozijn), sara.erasmus@wur.nl (S. Erasmus), d.fitzpatrick@ucc.ie (D. Fitzpatrick).

<https://doi.org/10.1016/j.foodres.2018.09.044>

Received 24 July 2018; Received in revised form 12 September 2018; Accepted 15 September 2018

Available online 24 September 2018

0963-9969/ © 2018 The Author(s). Published by Elsevier Ltd. This is an open access article under the CC BY-NC-ND license (<http://creativecommons.org/licenses/by-nc-nd/4.0/>).

into the deposit. The latter results in brines. For sea salt, salt is directly extracted from oceans/seas and saline lakes. For harvesting of crystals, brine and sea water may be subjected to either solar or artificial (heating, vacuum) evaporation. (EUsalt, 2017).

The total annual global production is around 250 million tonnes of salt (Statista, 2017). Although well-known as a food seasoning, most salt is nowadays actually used for non-food applications. Typical non-food applications include the production for the chemical industry, for de-icing of roads, softening of water and stabilization of road constructions. Its major industrial products are caustic soda and chlorine. Specifications for salt vary widely according to its intended use. Salt intended for food seasoning or preservation must unquestionably be much purer than road salt, but salt used for certain scientific purposes may need to be even purer. For most purposes, rock salt is allowed to have a grey, pink, or brown tinge rather than being pure white. The impurities that cause these colors may make up as much as 4% of a sample (Madehow, 2017). A food grade salt on the other hand should contain at least 97% sodium chloride according to Codex guidelines (1985). The price of salt depends on the type of salt, production location and product form: rock salt or brine. Salt brine is the least expensive since it is cost efficient to produce and processing is minimal. Vacuum pan salt is the most expensive because of the energy required for its production and the degree of final-product purity. Regional differences are also reported to occur, owing to labour rates, energy costs, transport, operating factors (Elzea Kogal, 2006). Yet, for culinary table salts the perceived sensory quality is sometimes also related to the provenance. Examples of these culinary table salts are the French *fleur de sel*, the Portuguese *Flor de Sal*, Hawaiian black lava sea salt, *Sel Marin de Guerande* grey sea salt (Celtic sea salt), pink Himalayan sea salt, Mayan salt, Peruvian pink salt, Bolivian rose salt, as well as the Atlantic – Australian – Balinese – Sicilian – Mediterranean salts (Macias, 2014; Wideopenats, 2017).

The prices of salt vary considerably and depend on their grade and origin added value. Various commercial sources on the internet show that road salt cost approximately € 0.08/kg; regular table salt ~€ 0.35/kg; simple Atlantic sea salt ~€ 1.20/kg; Himalayan pink salt ~€ 10/kg; Hawaii black salt ~€ 30/kg; Murray River salt from Australia or *Yuki Shio* salt from Japan ~€ 100/kg; and a culinary salt like '*Fumee de sel*' (traditionally smoked salt) retails at € 150/kg. These price differences drive adulteration of salts since they allow considerable illegal profits. Various cases have been identified. In the past substitution of food grade salt with industrial grade salt has been discovered, for instance in Poland (EU Parliament, 2013), in Iceland (Ministry of Fisheries and Agriculture of Iceland, 2012), and in China (SDA China, 2017). Some general salt adulteration cases also surfaced in Africa (Newvision, 2013) and Asia (E-pao, 2016).

Salts vary in their composition, which can be analysed by using different techniques, e.g. inductively coupled plasma mass spectrometry (Satyanarayanan et al., 2007) and neutron activation analysis (Steinhauser, Sterba, Poljanc, Bichler, & Buchtela, 2006). They have also been characterized with other – electromagnetic and light reflection and based -techniques, such as X-ray diffraction technology (Fernández-López et al., 2014), Raman spectroscopy (Weselucha-Birczyńska, Toboła, & Natkaniec-Nowak, 2008), scanning electron microscopy (Fernández-López et al., 2014), and combinations of microscopy and Raman spectroscopy (Toboła, 2018).

Different types of salt have their own crystalline shapes. For example, table salt, which is a combination of sodium and chloride ions, is more cube-shaped (face centred cubic). On the other hand, Epsom salt, which is a combination of magnesium and sulfate ions, is shaped like a prism. Therefore, the type of salt used to form crystals will result in forms reflective of that particular salt as water evaporates. Flake and dendritic forms of salt are also known. Dendritic salt is formed by evaporation of brines that contain small amounts (5 ppm) of ferrocyanide ions (Davidson & Slabaugh, 2003).

To date, acoustic properties of materials have hardly been used in food identity or authenticity studies so far, but they may be very useful considering the marginal sample preparation required and its rapid nature. Some groups have worked on sound resonance characteristics of powdered material though. They have established that the sound resonance characteristics of water will change when a powdered material is added to that water. This applies when chemical compounds (e.g. sodium carbonate, copper pentahydrate, tartaric acid (Fitzpatrick, Krüse, et al., 2012)), sucrose (Fitzpatrick et al., 2014), milk protein concentrate powders (Vos et al., 2016), or various pharmaceutical products are dissolved (Fitzpatrick, Scanlon, et al., 2012). This acoustic effect of air bubbles has been extensively reported by Crawford in the 1980s/1990s, and is also called the 'hot chocolate effect' (Crawford, 1982; Crawford, 1990). When such a compound is added to a liquid and dissolution starts, minute gas bubbles are generated in the liquid. This formation is due to entrained gases adhered to or trapped within the particles. It is therefore, affected by both the composition and the structure of the solute added. The instantaneous presence, generation and subsequent disappearance of these bubbles can be detected indirectly – real time – by monitoring an acoustic phenomenon associated with the sound velocity. The distribution of the solute reduces gas solubility further, resulting in additional gas bubbles, and increases total gas volume in the solution. The total bubble volume increases the compressibility of the solution, which results in a reduction of the velocity of sound. This effect can be monitored by the frequency change of acoustic resonances that are mechanically provoked in a solution. It measures indirectly the change in gas/bubble volume in the solution due to the addition of the powdered material (Fitzpatrick, Krüse, et al., 2012). The technique applied to measure these changes is Broadband Acoustic Resonance Dissolution Spectroscopy (BARDS).

Acoustic profiling may provide an interesting strategy to characterise salts of various origins to underpin their identity which in turn may be used for future authentication studies. The combination of the composition and the morphology of salt crystals, which are unique traits of salts from different origins, may be reflected in their acoustic properties. In the current study we evaluate food grade and technical grade salts for their unique acoustic resonance traits applying BARDS and we explore the impact of the composition and the particle size distribution of the salts to explain the phenomena observed.

2. Experimental

2.1. Materials

Sixty food grade and technical grade salt samples were purchased in various retail outlets across Europe (Table 1). The 50 food grade samples included basic salts, i.e. three regular table salts and three low sodium table salts, as well as culinary salts. The latter comprised eight colored salts (various colors), seven Himalaya salts (pink), 17 sea salts (white), and 12 specialty salts (white). The ten technical grade samples included five bath salts and five road salts. Samples were subjected to analysis in their intact form without further preparation and also after grinding to a fine powder for 30 s in a coffee grinder (Tristar KM-2270. Tristar, Smartwares Group, Tilburg, the Netherlands).

Three reference salts (for analysis grade) were used: NaCl (Merck, 1.06404), KCl (Merck, 1.04936) and MgCl₂ (Merck, 1.05833). The three salts were supplied by VWR International B.V. (Amsterdam, the Netherlands). MgCl₂ was dried over night at 103 ± 2 °C before use because of its highly hygroscopic nature. Mixtures of the salts were prepared: in the following NaCl/KCl and NaCl/MgCl₂ proportions: 1:4; 1:3; 1:2; 1:1; 2:1; 3:1; 4:1 (w/w). Furthermore, three way mixtures were prepared in the NaCl/KCl/MgCl₂ proportions: 1:1:1; 2:1:1; 3:1:1; 4:1:1; 1:2:1; 1:3:1; 1:4:1; 1:1:2; 1:1:3; 1:1:4 (w/w).

DeminerIALIZED water was used in all experiments.

Table 1
Sample specifications.

Grade	Category	Samples (origin of salt)	Number of samples	Price category				
				< 5€/kg	5–15€/kg	> 15€/kg		
Food grade	Basic salts	Table salts (white)	Table1-Table3 (EU)	3	2	1		
		Low sodium salts (white)	LowNa1-LowNa3 (EU and Pakistan)	3	2	1		
	Culinary salts	Colored salts (various colors)	Colored1&2: Lac rose, pink (Senegal)		2	2		
			Colored3: Kala namak black, heat treated in charcoal (India)		1		1	
			Colored4: Hawaii green (USA)		1		1	
			Colored5: Murray river, orange (Australia)		1 ^a		1 ^a	
			Colored6: Persian blue (Iran)		1		1	
			Colored7: Hawaii black (USA)		1		1	
			Himalaya1-Himalaya7 (Pakistan, unknown origin)		7	2	4	1
		Sea salts (white)	Sea1-Sea17 (Caribbean, EU, India, Israel, unknown origin)	17	6	5	6	
		Specialty salts (white)	Spec1: Zechsteinsee salt (Germany)		1	1		
			Spec2: Utah sweet salt (USA)		1		1	
			Spec3: Yuki Shio salt (Japan)		1 ^a		1 ^a	
			Spec4: Inca spring salt (Peru)		1		1	
			Spec5: Kalahari desert salt (Namibia)		1	1		
	Spec6: Spring water salt (Portugal)			1		1		
	Technical grade	Bath salts (various colors)	Bath1–5 (unknown origin)		5	5		
			Road salts (white/grey)	Road1–5 (unknown origin)	5	4	1	
		Food grade cumulated			50	14	14	22
			Technical grade cumulated			10	4	6

^a > 90€/kg.

2.2. Analysis of sodium and potassium content of salts

The sodium and potassium concentrations in the ground salts were measured using the flame photometry based method described in a national regulation of the Netherlands (Landbouwkwaliteitsregeling Annex IX, 1994; BWB XP Flame Photometer, Instrument Solutions Benelux, Nieuwegein, the Netherlands). The principle of the method is based on the initial conversion of cations of sodium and potassium into the atomic state when sprayed into a flame, which is followed by excitation of a small fraction of the atoms. Subsequent relaxation of the excited atoms to the lower energy level is accompanied by emission of light (photons) at characteristic wavelengths (Na: 589 nm, K: 766 nm). Intensity of the emitted light depends on the concentration of particular atoms in the flame, which was calibrated using a five point calibration set ranging from 0 to 4 mg Na/L or K/L. The salt samples were diluted with demineralized water to meet the appropriate measurement range (10–20 × dilution).

Considering that most sodium and potassium will be present as NaCl or KCl, concentrations NaCl and KCl were subsequently calculated considering that 1 g NaCl consists of 393 mg Na and 1 g KCl of 235 mg K. All samples were analysed in duplicate. Means were calculated as well as the coefficient of variation of the measurements according to the method for duplicate measurements of Hyslop and White (2009). The values were subsequently averaged to obtain the measurement variation value (CV% analysis). The means and coefficient of variation over the samples (CV% samples) were calculated as well for both NaCl and KCl, data which show the variation between samples in the sample group.

2.3. Particle size distribution measurements

The particle size distributions of both intact and ground samples were measured using a laser light diffraction analyzer, the Mastersizer

3000 in combination with the Aero S dry powder dispersion accessory (Malvern Instruments, Malvern, UK). The Aero S disperses dry samples by accelerating particles through a venturi with compressed air. The particles travel through the measurement cell of the Mastersizer 3000 using a vacuum source. For this study, an air pressure of 2 bar was maintained during sample dispersion. A sample of (approximately 10 g) was loaded into the hopper (3 mm gap) which was positioned on a general purpose sampler tray. A sample feed rate of 20% through the Aero S was maintained using a vibrating feeder. The feed rate was only adjusted (not > 40%) if the samples were clumpy or sticky to insure consistent flow. Measurement of each sample only commenced once the obscuration was in range with a lower limit of 0.5% and a higher limit of 6%. The non-spherical particle mode and Fraunhofer type was selected as the particle type. The particle size distribution was monitored during each measurement and expressed as Dx (50), the median; Dx (90), the point at which 10% of the population resides above this point and 90% resides below this point; D[4,3], the mean diameter over volume (De Brouckere mean); and D[3,2], the volume/surface mean (Sauter mean). Three replicate measurements of each salt were carried out. The coefficient of variation was calculated for each salt and parameter, and the values were subsequently averaged to obtain the measurement variation value (CV% analysis). The means and coefficient of variation over the samples (CV% samples) were calculated as well, which show the variation between samples in the sample group.

2.4. BARDS analysis

2.4.1. Theoretical background of BARDS

The acoustic properties of liquids are influenced by dissolved gas present in the liquid phase. Generally the presence of gas will reduce the speed of sound. When compressible gas bubbles are introduced or generated in a liquid due to dissolution of a compound, the compressibility of the solution will change. The altered compressibility will

affect the speed of sound and this results in frequency changes of induced acoustic resonances in the solution. Either in air or liquid phase, the sound velocity (v) in a medium (m s^{-1}) is described by Eq. (1).

$$v_{(\text{sound})} = \sqrt{\frac{1}{K \cdot \rho}} \quad (1)$$

where ρ is the density (kg m^{-3}) and K is the compressibility of the medium (Pa^{-1}). The density is hardly affected by the micro bubbles formed by dissolution of for instance salt crystals, but the compressibility of the solution is considerably increased by their generation/introduction. The net effect is a significant reduction of the velocity of sound in the solution. The relationship between the sound velocity and the fractional bubble volume was derived by Crawford (1982), and is given in Eq. (2):

$$v_w/v = \sqrt{(1 + 1.49 \cdot 10^4 \cdot f_a)} \quad (2)$$

where v_w and v are the velocities of sound (m s^{-1}) in pure water and water with bubbles, respectively, and f_a is the fractional volume occupied by the air bubbles. BARDS analysis focuses on the fundamental resonance mode of the solution. The fundamental resonant frequency is determined by the sound velocity in the solution and the approximate but fixed height of the liquid level, see Eq. (3):

$$\text{freq} = \frac{\text{freq}_w}{\sqrt{1 + 1.49 \cdot 10^4 \cdot f_a}} \quad (3)$$

where freq_w and freq are the resonance frequencies (kHz) of the fundamental resonance modes in pure water and water with bubbles, respectively. The frequency change reflect changes in the velocity of sound and thus the bubble volume generation/introduction, which in turn is affected by the salt crystals' composition and structure. Principles and underlying mechanisms have been detailed by Fitzpatrick, Krüse, et al. (2012).

2.4.2. BARDS equipment

The BARDS spectrometer (BARDS Acoustic Science Labs, Cork, Ireland) consisted of a chamber with a dissolution vessel (borosilicate), microphone (Sony ECM-CS10, range 100 Hz–16 kHz), a magnetic stirrer and follower as described by Vos et al. (2016). At the front, the dissolution chamber is accessed to place the glass dissolution vessel and the top can be accessed to place a powdered sample in a weighing boat. The boat allows automatic introduction of the salt. The microphone was positioned above the top of the glass within the chamber. The glass vessel, containing the demineralized water, was placed on the stirrer plate and a magnetic stirrer tapped gently the inner vessel wall. The stirrer acts as a source of broadband acoustic excitation, thereby inducing various acoustic resonances in the glass, the liquid and the air column above the liquid. The audio was sampled at a rate of 44.1 kHz. A fast Fourier transform was applied to the signal, resulting in a typical BARDS frequency response and the resonances recorded in a frequency band of 0–20 kHz. The frequency response was measured during the dissolution of each salt sample in water.

2.4.3. BARDS experimental procedure

For the acoustic measurements of the salts 0.8 g intact or ground salt and 25 mL of demineralized water was used resulting in a final concentration of 32 g salt/L water (0.55 M). This concentration is below the NaCl and KCl salts solubilities in water, which are approximately 4 and 6 M at room temperature, respectively (Bharmoria, Gupta, Mohandas, Ghosh, and Kumar (2012)). The salt experiments were carried out at ambient temperature (22 °C) and atmospheric pressure. Gas oversaturation of demineralized water prior to introduction of the powders was removed through agitation by shaking vigorously for 60 s and then resting for 10 min. Otherwise, remaining gas oversaturation may lead to an over-response (Fitzpatrick et al., 2013).

Before the introduction of the salt crystals to the water, the

spectrometer recorded the steady state resonances of the system for 30 s after the stirrer was set in motion. The steady-state frequency before addition of the powder is designated as the 'volume line', so called as it varies depending on the liquid volume in the vessel. Subsequently the salt was automatically introduced and the acoustic profiles recorded for 400 s. All measurements were carried out in triplicate.

2.4.4. BARDS data analysis

In the BARDS experiments, the frequency-time response of the fundamental resonance was manually extracted from the total acoustic response. These acoustic profiles were transferred to a spreadsheet resulting in a data matrix of 60 replicated samples (rows) and 50 frequencies (variables, columns). For three samples (Sea3, Sea4 and Colored1), where the acoustic signal was too weak for annotation in the first 0–20 s after addition of the salt, row-wise interpolation was applied using a spline interpolation polynomial. Means, standard deviations and coefficients of variation were calculated for the acoustic profiles of each sample ($n = 3$). The maximum frequencies and time to this maximum were extracted from the acoustic profiles. The coefficient of variation was calculated for each salt over the three replicates of a measurement, and the values were subsequently averaged to obtain the measurement variation (CV% analysis). This number provides information on the reproducibility of the measurements over the group of samples. The means and coefficient of variation over the samples (CV% samples) were calculated as well, which shows the variation across samples in the sample group.

Correlations between these acoustic profile parameters and Na and K contents as well as between the acoustic profile parameters and particle size distribution parameters were calculated using Pearson correlation coefficients (Snedecor & Cochran, 1980).

3. Results and discussion

3.1. Acoustic characteristics of food grade and technical grade salts

The 60 salt samples were subjected to BARDS analysis and the frequency-time course of the resonance curves (acoustic profiles) were acquired. Mean acoustic profiles for the food grade salts, as well as the road salts and the bath salts are shown in Fig. 1. The figure shows acoustic profiles and the various stages during dissolution of the salts. The first 30 s of the measurements, the acoustic frequencies of the vessel remain steady until the salt sample is added to the water in the vessel. The first 30 s represent the resonance of the glass vessel as it is induced to resonate by the magnetic stirrer. This volume line frequency depends on the liquid level of the solvent (water) in the vessel. After addition of the salt sample the initial resonant frequency of 9.2 kHz declines quickly to a level of 6–8 kHz ($F_{\text{min_intermediate}}$), the latter depending on the type of sample. For bath salts, a further gradual decrease is observed, whereas food grade and road salts show an initial increase after the first sharp decline to a frequency maximum ($F_{\text{max_intermediate}}$), and subsequently a gradual decrease until a final frequency minimum (F_{min}) is reached.

During the course of the measurement, the change in resonance

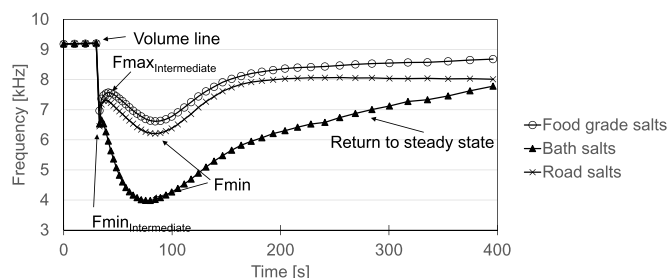


Fig. 1. Mean acoustic profiles of three categories of salts dissolved in water.

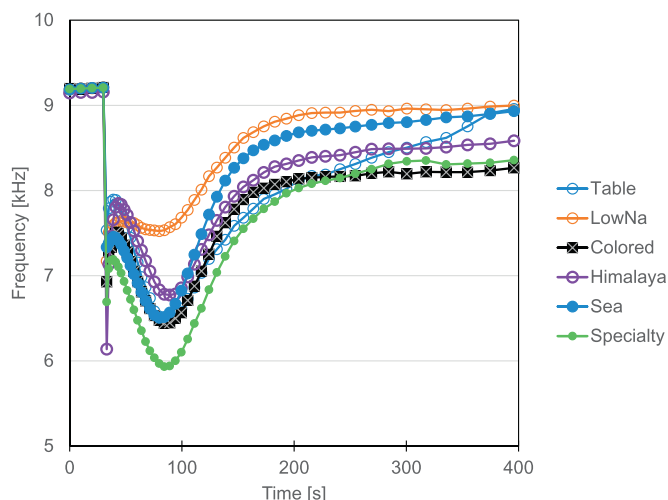


Fig. 2. Mean acoustic profiles of various groups of food grade salts dissolved in water.

frequency is the net effect of change of the compressibility of the solution due to (1) released gas bubbles which were adhered to the particles, (2) the gradual release of gas due to dissolution of the salts, and (3) the release of gas into the surrounding air phase (bubbles escaping from the liquid phase). In the first phase, after the introduction of the samples gas bubbles loosely adhered to the salt particles are instantly

released into the solution. This stage is reflected by the sharp initial frequency decrease. In addition to the rapid release of gas bubbles adhered to the salt particles, a second process occurs at a different rate, i.e. the dissolution of the salts which results in an additional gradual release of the gas trapped within the porous particles. The increased gas concentration in the solution, will favour transfer of gas over the liquid/air surface to the surrounding air in order to restore equilibrium (Henry's law). Therefore, the measured frequency is the net result of gas formed and gas bubbles escaping from the liquid, which may result for some samples in a frequency increase after the initial sharp decline. At some stage gas oversaturation in the solution may occur, which accelerates transport of the gas to the air phase. Fmin of the BARDS response represents an equilibrium between the rate of formation of gas in solution and the rate of liberation of gas from the surface of the solvent. At this stage, the solution is at its most compressible. After the minimum, the resonance frequency returns gradually to steady state due to transfer of gas at the surface into the surrounding air.

The dissolution rate is determined by both the composition of the salts as well as the physical structure of the crystals since the particle size surface area of the crystals affects dissolution rates considerably. During dissolution the concentration of dissolved salts will increase in the solution, which affects the gas solubility in the solution. In general, gas solubility will decrease with higher salt concentrations. In this experiment a final concentration of 32 g salt/L demineralized water is reached for all samples, but the composition and the morphology of the salts vary. The BARDS response curves reveal the similarity of the mean curves of the food grade and road salts, whereas the mean bath salts curve deviates strongly from the other two because of the lack of

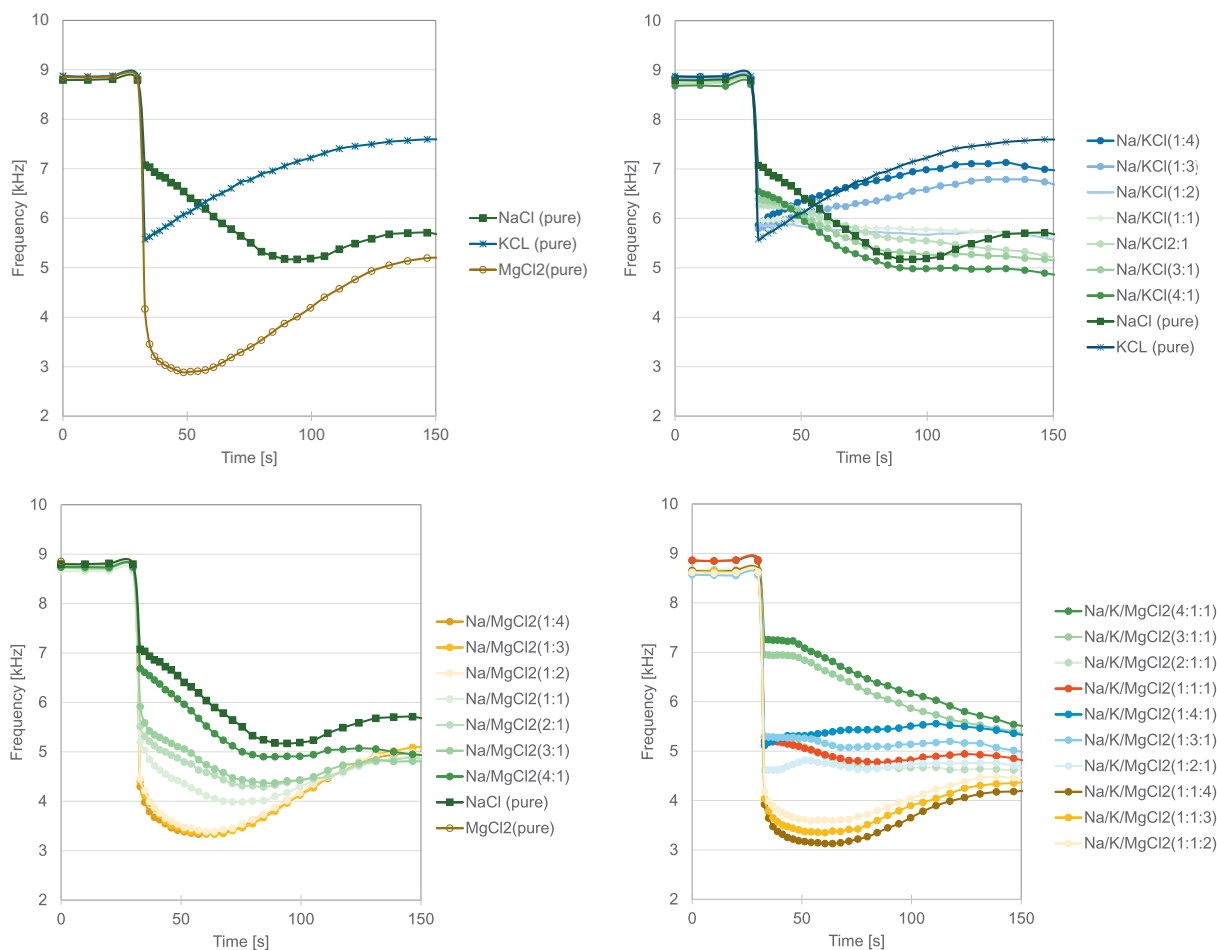


Fig. 3. Acoustic profiles of reference salts and mixtures thereof dissolved in water: individual salts (3–1); NaCl/KCl mixtures (3–2); NaCl/MgCl₂ mixtures (3–3); NaCl/KCl/MgCl₂ mixtures (3–4).

Table 2
Composition of salts.^a

	NaCl	KCl	Others
	[% w/w]	[% w/w]	(calculated) [% w/w]
Table1	94	0	6
Table2	95	0	5
Table3	95	0	5
LowNa1	35	63	2
LowNa2	32	31	37
LowNa3	62	23	15
Colored1	95	0	5
Colored2	96	0	4
Colored3	93	1	6
Colored4	98	0	2
Colored5	96	0	4
Colored6	64	34	2
Colored7	92	0	8
Himalaya1	93	0	7
Himalaya2	94	1	5
Himalaya3	95	0	5
Himalaya4	98	0	2
Himalaya5	100	0	0
Himalaya6	94	0	6
Himalaya7	94	0	6
Sea1	96	0	4
Sea2	94	0	6
Sea3	96	0	4
Sea4	86	0	14
Sea5	95	0	5
Sea6	97	0	3
Sea7	94	0	6
Sea8	93	0	7
Sea9	88	0	12
Sea10	95	0	5
Sea11	94	0	6
Sea12	96	0	4
Sea13	96	0	4
Sea14	95	0	5
Sea15	92	0	8
Sea16	93	0	7
Sea17	92	0	8
Spec1	96	0	4
Spec2	93	0	6
Spec3	26	1	73
Spec4	91	0	9
Spec5	93	0	7
Spec6	92	0	8
Spec7	90	0	10
Spec8	97	0	3
Spec9	99	0	1
Spec10	96	1	3
Spec11	94	0	6
Spec12	100	0	0
Spec13	97	0	3
Bath1	92	0	8
Bath2	91	0	9
Bath3	94	0	6
Bath4	94	0	6
Bath5	1	1	98
Road1	95	0	5
Road2	88	0	12
Road3	86	0	14
Road4	91	0	9
Road5	92	0	8
CV% analysis	1	1	-
CV% samples	22	391	-

^aCalculated NaCl and KCl concentrations based on Na and K measurements.

^bCalculated over samples with measured contents > 0.

Table 3
Particle size distribution of intact salt samples.^a

	Sample Name	Dx (50)	Dx (90)	D [4,3]	D [3,2]	
		[μm]	[μm]	[μm]	[μm]	
Food grade	Table1	587	1047	635	493	
	Table2	413	693	437	352	
	Table3	475	788	504	409	
	LowNa1	441	730	474	411	
	LowNa2	467	768	496	413	
	LowNa3	1115	2070	1235	945	
	Colored2	695	1539	807	456	
	Colored3	398	662	422	331	
	Colored6	1115	2070	1235	945	
	Colored7	1481	2508	1595	1374	
	Colored1,4,5	NA ^b				
	Himalaya1	602	1041	648	512	
	Himalaya2-4	NA ^b				
	Himalaya5	819	1412	890	749	
	Himalaya6	748	1270	801	643	
	Himalaya7	799	1384	858	673	
	Sea1	1237	2253	1354	1052	
	Sea5	220	340	231	197	
	Sea6	520	861	555	474	
	Sea7	1023	1978	1147	857	
	Sea8	523	1041	572	344	
	Sea10	691	1251	744	522	
	Sea12	470	725	487	402	
	Sea13	1404	2420	1528	1312	
	Sea17	1490	2504	1607	1398	
	Sea2-4,9, 11,14-16	NA ^b				
	Spec2	511	816	542	478	
	Spec4	1225	2224	1350	1100	
	Spec5	484	967	521	238	
	Spec6	1083	2002	1199	933	
	Spec7	164	319	180	114	
	Spec9	850	1369	907	799	
	Spec10	67	165	85	16	
Spec11	690	1319	747	440		
Spec12	540	948	580	450		
Spec13	1428	2466	1536	1254		
Spec1,3,8	NA ^b					
Tech- nical grade	Bath1-5	NA ^b				
	Road1	355	588	375	295	
	Road2-5	NA ^b				
Refer- ence	NaCl	414	644	431	366	
	KCl	313	538	331	247	
	MgCl	151	357	175	59	
	CV% analysis commercial salts	2	2	2	3	
	CV% samples commercial salts	53	53	53	59	

^aSample specifications in Table 1.

^bNA = not available, beyond instrument specifications.

$F_{\text{min-intermediate}}$ and $F_{\text{max-intermediate}}$ and a lower F_{min} in comparison to the other two groups. This first part of the process is obviously masked by a rapid evolution of gas. The acoustic profile depends on the physicochemical properties of the solute. In this case, the presence of surfactants in the bath salts are likely to favour rapid dissolution, affects gas solubility of the solution and can affect the rate of gas bubbles lost at the surface.

The acoustic profiles of the six types of food grade salts exhibit similarity (Fig. 2), but also some distinct differences. The regular table salts show a more general pattern representing more or less the mean of all salt groups, but the LowNa salts show a more rapid return to the steady state, whereas in particular the specialty salts show a low

frequency value at F_{min} . Although the sea salt group showed a similar F_{min} drop as the colored salt group, it has a faster return to the steady state.

3.2. Acoustic characteristics of reference salts

For comparison, the three reference salts were subjected to BARDS analysis too, the mean acoustic profiles of which are shown in Fig. 3. The NaCl, KCl and MgCl_2 samples show very distinct profiles in the first 150 s. NaCl shows a gradual decrease to F_{min} and a U-shaped F_{min} after 90 s, whereas KCl shows a V-shaped F_{min} after 35 s (Fig. 3-1). The latter shapes agree with results in previous studies (Fitzpatrick et al.,

Table 4
Particle size distribution of intact and ground salt samples.^a

Sample	Coarse or Fine	Dx (50)	Dx (90)	D [4,3]	D [3,2]
		[μm]	[μm]	[μm]	[μm]
Table1	Intact	587	1047	635	493
	Ground	81	234	106	17
LowNa3	Intact	1115	2070	1235	945
	Ground	75	241	105	17
Colored2	Intact	695	1539	807	456
	Ground	67	337	141	24
Himalaya5	Intact	819	1412	890	749
	Ground	61	177	81	15
Sea7	Intact	1023	1978	1147	857
	Ground	187	670	283	101
Spec4	Intact	1225	2224	1350	1100
	Ground	290	813	377	158
CV% analysis	Intact	3	2	2	4
CV% samples	Intact	27	26	27	33
CV% analysis	Ground	3	3	3	3
CV% samples	Ground	73	64	66	109

^aSample specifications in Table 1.

2013). MgCl_2 results in a very steep initial decline (considerable down slope value) and low U-shaped F_{min} at around 50 s. All three salts show a maximum around 150 s which is followed by a gradual decrease in frequency. This is most likely due to bubble formation at the wall of the glass flask which is formed with this kind of pure salts when oversaturation occurs, and which are released at a later stage (Fitzpatrick et al., 2013). Hence, only the first 150 s of the curves are considered.

The acoustic profiles of the NaCl/KCl (Fig. 3-2) and NaCl/ MgCl_2 mixtures (Fig. 3-3) show a gradual transition from one reference salt to the other. For the NaCl/KCl mixtures the fundamental curve undergoes a transition from U-shape (high NaCl) to V-shape (high KCl). The V-shape is observed when an excess of KCl is present. F_{min} converges in terms of magnitude and time when KCl is present in excess. This means that KCl is dominating the curve in that situation. The time to F_{min} (Δt) is decreasing with increasing KCl concentrations when Na is present in excess.

The fundamental curves of the NaCl/ MgCl_2 mixtures exhibit a similar U-shape, but the F_{min} changes from 5 KHz to 3.3 KHz with increasing concentrations of MgCl_2 , and Δt decreases. MgCl_2 is dominating the curve shape when an excess of MgCl_2 is present, i.e. from the NaCl/ MgCl_2 1:2 ratio, when the frequency minimums begin to converge.

When the three salts are present excess of NaCl, KCl and MgCl_2 result in F_{min} s of 7, 5 and 3.5 kHz, respectively (Fig. 3-4). When one of the salts is present in excess, it dominates the curve with limited effect of its further increasing concentrations on F_{min} magnitude and Δt .

3.3. Sodium and potassium composition of the salts

The 60 commercial salt samples varied in grade and origin, and some had distinct colors, such as green, orange, pink, black, blue, etc. which indicate differences in composition (Table 1). According to their labels, the food grade salts consisted primarily of NaCl, with small fractions of Ca, Mg, K, Fe and Zn being present as well except for the LowNa salts. Although the food grade salts and the road salts predominantly consisted of minerals according to their labels, the bath salts constituents included surfactants and odorants as well.

The NaCl and KCl concentrations were determined in all salts (Table 2). Means and CV% analysis and CV% samples were calculated for each salt. NaCl concentrations varied between 1 and 100% w/w. Most of the food grade salts comprised 90–100% w/w NaCl, except for the three LowNa salts and two culinary salts (Colored6 and Spec3). The KCl concentrations were generally low, except for the three LowNa salts and culinary salt Colored6. In most cases, remaining constituents made up < 10% w/w of the salt. Two of the three LowNa salts showed higher fractions ($\geq 10\%$ w/w) of other constituents (MgCl_2 according to the packaging label) as well as the samples Sea4 (14% w/w), Sea9 (12% w/w), Spec3 (73% w/w) and Spec7 (10% w/w) (Table 2). One Himalaya salt and one specialty salt consisted surprisingly of only NaCl (100% w/w). For the technical grade salts, only three samples showed higher fractions of other constituents: Bath5 (98% w/w), Road2 (12% w/w) and Road3 (14% w/w).

3.4. Particle size distributions of the salts

The particle size distributions were determined for all salt samples, the results are listed in Table 3. A number of salts were out of spec for the measurements and blocked the entrance of the instrument. Hence, it was not possible to determine their particle size distributions. However, the distributions of 33 samples were measured. The Dx 50 values varied from 67 to 1490 μm , and the Dx 90 values of nine of the measured samples were 1000 μm or over and 11 were below 500 μm .

From each sample group one representative salt was measured both in its intact and ground form (Table 4). The median particle size (Dx 50) decreased by a factor of nine on average after grinding. Grinding results also in narrower (absolute) distributions as well as in an enormous increase of particle surface area, as shown by the reduction of the volume/surface mean (D[3,2]) by a factor of 30 on average.

3.5. Acoustic profiles of salts considering their composition and particle size distributions

For comparison, Eq. (3) was applied to the raw BARDS acoustic profiles to generate data relating to the fractional gas volume occupied

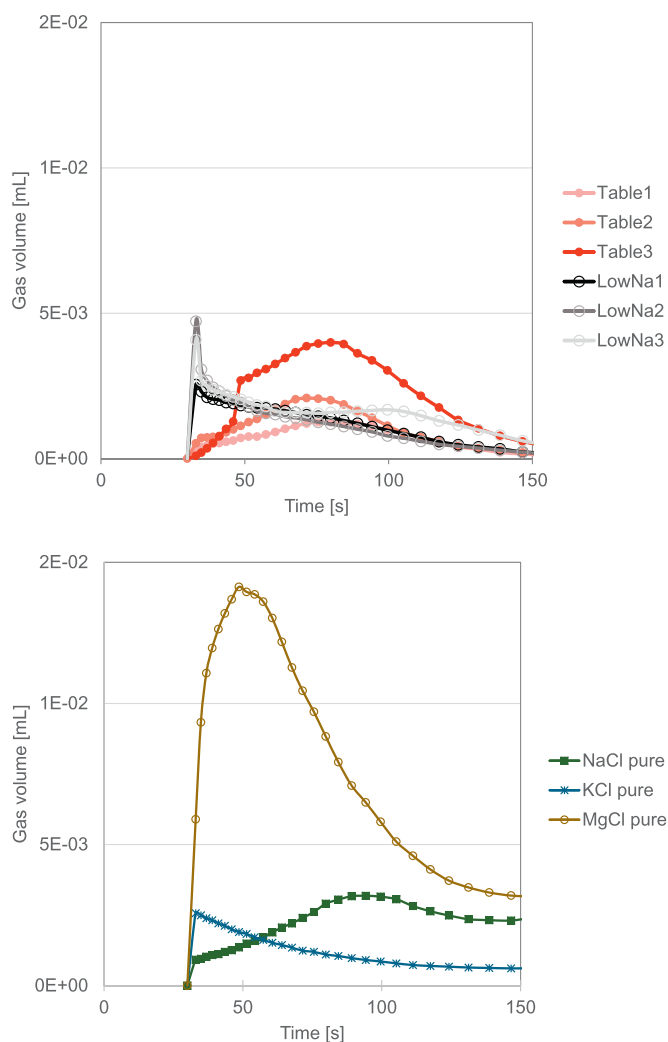


Fig. 4. Gas volume plots of basic salts (upper) and reference (lower) salts.

by compressible gas during the dissolution of the commercial salts and reference salts. The gas volume plots presented in the following sections concern absolute volumes.

3.5.1. Compositional effects

In order to evaluate compositional effects, the gas volume plots of the intact basic salts, i.e. table salts and LowNa salts, were generated together with those of the three reference salts (Fig. 4). Since the six commercial salts have similar particle size distributions except for sample LowNa3 (Table 3), the differences in gas generation observed are primarily due to compositional differences. The initial up-slope in the plots indicated the rate at which gas was released and generated from the salt samples. The data suggest a considerable difference in dissolution behaviour between table and LowNa salts, the latter of which comprised higher levels of non-NaCl constituents. LowNa salts exhibited a very rapid release of gas, the disappearance of which from the water began immediately and proceeded rapidly. Conversely, there was a more gradual increase in the gas volume to a higher maximum observed for the table salts, after which gas volume remained constant in the system for ~20 s, due to a balance of gas release/generation and disappearance, before gas disappearance from the liquid surface became dominant. The gas generation observed follows the patterns of those of the reference salts. The very rapid initial release is

characteristic of KCl, whereas a more gradual increase and subsequent decrease is seen for NaCl. Studies have shown that dissolution rates of KCl are higher than those of NaCl in water (Simon, 1981). The magnitude of the maximum gas volume in the solution was lower for sample LowNa1 compared to the other two LowNa samples. LowNa1 differed in composition since it comprised predominantly NaCl and KCl, whereas the two others constituted of a considerable fraction of additional compounds (including $MgCl_2$ according to the packaging label). LowNa3 consisted of 2/3 of NaCl which may explain the second maximum observed around 100 s, characteristic of the NaCl pattern.

3.5.2. Particle size effects

A variety of intact salts showed a rapid initial release of gas (Fig. 5-1) and they comprise either higher fractions of non-NaCl constituents (Spec3), are of a coarser nature (Colored5, Sea11, Sea13, Sea17, Spec8 and Spec13) or both (Sea9). Another group of the sample set exhibit a more gradual release of gas from the salt samples (Fig. 5-2) and subsequent gradual release from the solution consist of finer intact salts (LowNa1-LowNa3). In the coarser material more gas is entrained which is released nearly instantly when the salt particles touch the water. It is interesting to note that the pattern of Spec3 (the *Yuki Shio* salt from Japan) is different from the rest – likely due to its higher content of additional compounds (73% w/w).

The gas volume plots of a set of samples with NaCl content over 90%, the sea salts (Sea1-Sea17), were compared for both the intact salts and the ground material to evaluate the effect of artificial particle size reduction (Fig. 5-3 and 5-4, respectively). From these plots it appears that gas volume curves become much more similar after grinding.

3.5.3. Compositional versus particle size effects

To compare the effects of the salts' composition and the size of their particles, the maximum gas volumes in the solutions were calculated which are listed together with the time to reach these maximums for all salts (Δt), in intact and ground state in Table 5. The maximum gas volumes were correlated with the NaCl and KCl contents of the salts. For the intact salt this resulted in Pearson correlation coefficients of 0.01 ($P = .93$) and -0.06 ($P = .77$) for NaCl and KCl, respectively, and for the ground salts in coefficients of 0.06 ($P = .65$) and -0.10 ($P = .43$). Thus, no significant correlations were observed for the maximum gas volume values and the mineral composition of the salts.

Similarly, correlation coefficients were determined for the time to reach the maximum gas volumes (Δt) and NaCl and KCl contents of the salts. For the intact salts the coefficient is 0.26 ($P = .04$) for NaCl and -0.16 ($P = .21$) for KCl, and for the ground salts these values are 0.48 ($P = .0001$) and -0.38 ($P = .00032$), respectively. Thus, a relationship between the temporal aspects and the salt composition exists, which is stronger when salts are ground.

For the intact samples, the Pearson correlation coefficient was also calculated for the maximum values and particle size parameters. The correlation was not significant, i.e. for the maximum values and $D_x 50$, the value was 0.22 ($P = .09$) and for $D_x [4,3]$ 0.21 ($P = .10$). However, a strong correlation was observed between the time to maximum values (Δt) and particle size parameters, with a correlation coefficient of -0.54 ($P < -0.00001$) for both $D_x 50$ and $D_x [4,3]$. This shows that for intact salts the time to reach the maximum gas volume in solution (Δt) is significantly affected by the particle size distribution. Hence, the coarser the salt, the faster the maximum is reached (smaller Δt). Furthermore, the time is affected by the salt composition as well, the more NaCl present the longer it will take to reach the maximum (larger Δt), but this effect is more significant with ground material in which particles are smaller and more similar in size. The latter is evident from Table 5 for the ground salt samples (LowNa1-LowNa3, Colored6, Sea4, Sea9, Spec3, Spec7, Bath5, Road2 and Road3) which contained a higher percentage of non-NaCl constituents (Table 2). The maximum gas

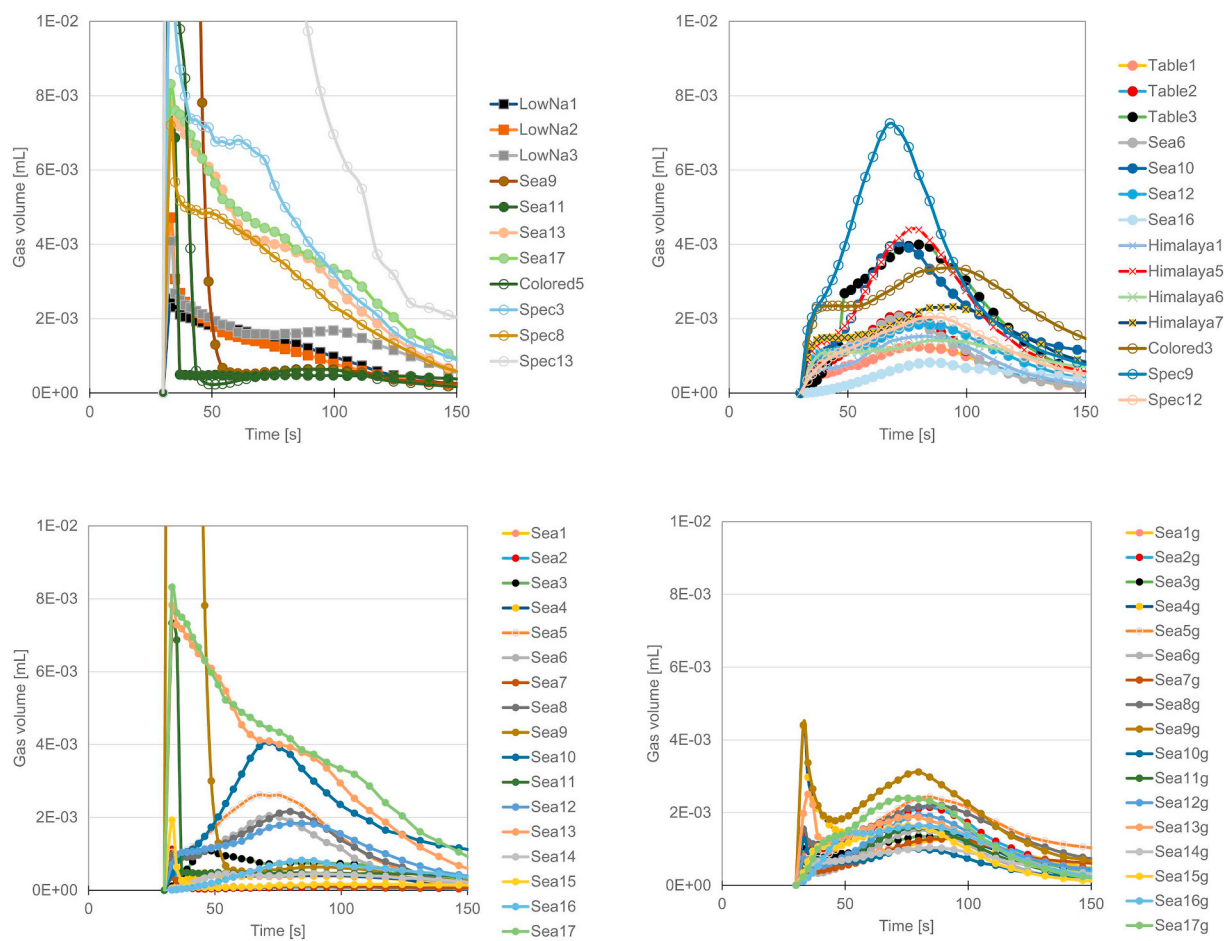


Fig. 5. Gas volume plots of intact coarser (5–1) and finer (5–2) salts, and intact (5–3) and ground (5–4) sea salts.

volume is not significantly affected, by the salt composition nor by the particle size of the salt. Therefore, it is primarily the rate at which gas is released that is affected by the size of the particles. Only when the particles are more similar in size, the composition also starts playing a role in its release rate.

Thus, both composition and morphology of the salt crystals are important as they determine the rate of gas release characteristics and thus acoustic traits of salts. Coarse salts with high levels of non-NaCl constituents will release gas rapidly and result in a rapid change in sound frequency. Conversely, fine salts composed of pure NaCl exhibit a slower release rate and a slower change in sound frequency.

Generally KCl dissolves more rapidly in water than NaCl (Simon, 1981). However, the presence of components other than NaCl may also affect the morphology of the crystals. The culinary salts (Colored, Himalaya, Sea, Specialty salts) with NaCl and other salts present most likely comprise single and mixed polycrystalline particles with both NaCl and for instance KCl because they have crystallized simultaneously. This is unlike the mixtures of the reference salts, where different single composition crystals were mixed. Studies have shown that during simultaneous crystallization of NaCl and KCl from aqueous solutions by batch wise evaporation only NaCl crystallizes by molecular crystal growth, agglomeration, and secondary nucleation in the early stages. When the eutonic condition is exceeded, a KCl primary nucleation event takes place in solution. Subsequently, part of the resulting KCl particles agglomerate with the NaCl particles. Furthermore, epitaxial growth of KCl upon NaCl crystals takes place. Consequently, the end product comprises mixed composition polycrystalline particles

and single composition crystals of each salt. Evidently, these processes are sensitive to crystallization conditions such as evaporation rate, seed size, and seed content (Penha, Zago, Nairyoshi, Bernardo, & Seckler, 2018). The presence of other kinds of molecules will affect the crystal growth and the structure and morphology of the crystals. Small amounts of impurities are frequently observed to inhibit the growth of crystals. For this inhibition, impurity species are considered to act as obstacles on the surface of a crystal during the displacement of growth steps. This may result in a weakened crystalline structure, which disintegrate more rapidly when in contact with water and favours subsequent dissolution.

Despite the fact that fine salts have a larger surface area, coarser salts show a more rapid release of gas. This may be due to the entrained gas that is rapidly released.

4. Conclusions

Listening to a variety of salts by BARDS resulted in distinct acoustic profiles for each of the salts. These distinct profiles are the result of release of entrained and dissolved gas upon dissolution of the salts, which is clearly affected by the composition of the salts, their morphology and the interaction of both. Current results show that the identity of salts can be described by their acoustic traits. This may be developed further in the future for verification of the identity of salts and even their authenticity of origin, while this technique also holds great potential to be extended to other powdered products.

Table 5
Gas volumes maxima and time to maxima from acoustic profiles of intact and ground salt samples.

	Sample Name	Intact samples		Ground samples	
		Max (mL)	Time to max (s)	Max (mL)	Time to max (s)
Food grade	Table1	1,3E-03	76	1,7E-03	89
	Table2	2,1E-03	72	1,7E-03	80
	Table3	4,0E-03	80	2,7E-03	89
	LowNa1	2,5E-03	33	7,2E-04	33
	LowNa2	4,7E-03	33	6,9E-04	33
	LowNa3	4,1E-03	33	2,2E-03	33
	Colored1-	5,8E-04	54	1,5E-03	89
	Colored2	2,4E-03	72	2,5E-03	33
	Colored3	3,4E-03	89	2,3E-03	89
	Colored4	1,1E-03	33	2,6E-03	76
	Colored5	1,8E-02	33	3,1E-03	84
	Colored6	1,8E-03	76	2,4E-03	33
	Colored7	3,6E-04	64	6,4E-04	76
	Himalaya1	1,5E-03	80	4,4E-03	33
	Himalaya2	4,1E-04	33	3,4E-03	33
	Himalaya3	7,5E-04	33	1,4E-03	80
	Himalaya4	3,8E-04	33	1,8E-03	33
	Himalaya5	4,4E-03	76	3,9E-03	33
	Himalaya6	1,4E-03	84	1,4E-03	84
	Himalaya7	2,3E-03	94	1,1E-03	84
	Sea1	9,3E-04	33	1,3E-03	94
	Sea2	1,1E-03	33	2,1E-03	84
	Sea3	1,1E-03	33	1,3E-03	80
	Sea4	4,8E-04	46	4,4E-03	33
	Sea5	2,6E-03	68	2,4E-03	84
	Sea6	2,1E-03	72	1,5E-03	80
	Sea7	3,6E-04	33	1,3E-03	94
	Sea8	2,2E-03	80	2,2E-03	89
	Sea9	5,3E-02	33	4,4E-03	33
	Sea10	4,1E-03	72	1,3E-03	33
	Sea11	7,3E-03	33	1,6E-03	76
	Sea12	1,8E-03	80	1,9E-03	80
	Sea13	7,8E-03	33	2,5E-03	35
	Sea14	4,6E-04	89	1,0E-03	84
	Sea15	1,9E-03	33	1,6E-03	76
	Sea16	8,2E-04	84	1,6E-03	80
	Sea17	8,3E-03	33	2,4E-03	76
	Spec1	4,5E-04	33	1,8E-03	84
	Spec2	1,0E-03	94	2,1E-03	89
	Spec3	1,3E-02	33	7,0E-03	33
	Spec4	9,4E-04	54	1,6E-03	89
	Spec5	2,1E-03	76	2,1E-03	89
	Spec6	7,7E-04	33	1,5E-03	80
Spec7	1,3E-03	80	1,5E-03	89	
Spec8	7,2E-03	33	3,0E-03	89	
Spec9	7,3E-03	68	1,7E-03	84	
Spec10	1,9E-02	64	1,3E-03	100	
Spec11	9,1E-03	33	4,4E-03	76	
Spec12	2,0E-03	84	2,1E-03	89	
Spec13	4,8E-02	33	2,0E-02	33	
Tech-nical grade	Bath1	1,4E-02	111	3,2E-02	72
	Bath2	1,5E-02	118	3,1E-02	76
	Bath3	1,2E-03	94	1,0E-02	76
	Bath4	2,9E-03	118	1,0E-02	84
	Bath5	9,9E-04	33	6,6E-04	33
	Road1	4,6E-03	76	3,5E-03	84
	Road2	1,5E-03	33	2,1E-03	33
	Road3	8,3E-04	33	4,1E-03	33
	Road4	7,1E-04	94	1,5E-03	94
	Road5	3,0E-03	118	2,4E-03	80
Mean	5,2E-03	60	3,7E-03	69	
CV%	183	45	158	35	

^aSample specifications in Table 1.

^bNA = not available, beyond instrument specifications.

Acknowledgements

The authors acknowledge financial support by the Ministry of Agriculture, Nature and Food Quality of the Netherlands. The sponsor was not involved in the study design; in the collection, analysis and interpretation of data; in the writing of the report; and in the decision to submit the article for publication.

References

- Aquilano, D., Otálora, F., Pastero, L., & García-Ruiz, J. M. (2016). Three study cases of growth morphology in minerals: Halite, calcite and gypsum. *Progress in Crystal Growth and Characterization of Materials*, 62, 227–251.
- Bharmoria, P., Gupta, H., Mohandas, V. P., Ghosh, P. K., & Kumar, A. (2012). Temperature invariance of NaCl solubility in water: Inferences from salt-water cluster behavior of NaCl, KCl, and NH₄Cl. *The Journal of Physical Chemistry B*, 116, 11712–11719.
- Braitsch, O. (1971). *Salt deposits, their origin and composition*. Berlin Heidelberg: Springer Verlag. <http://www.springer.com/us/book/9783642650857>.
- Codex Guidelines (1985). *Codex standard for food grade salt*. Codex Stan150–1985. http://www.codexalimentarius.net/download/standards/3/CXS_150e.pdf Accessed 17 June 2018.
- Crawford, F. S. (1982). The hot chocolate effect. *American Journal of Physics*, 50(5), 398–404.
- Crawford, F. S. (1990). Hot water, fresh beer, and salt. *American Journal of Physics*, 58(11), 1033–1036.
- Davidson, C. F., & Slabaugh, M. R. (2003). Salt crystals – Science behind the magic. *Journal of Chemical Education*, 80(2), 155.
- Elzea Kogal, J. *Industrial minerals and rocks: Commodities, markets, and uses*. (2006). <https://books.google.nl/books?id=zNiedkuule4C&pg=PA808&lpg=PA808&dq=price+industrial+grade+and+food+grade+salt&source=bl&ots=Nkndx1z9va&sig=b5zl9d4T1qZNhu6k5HAUJKkO8go&hl=en&sa=X&ved=0ahUKEwj70JOMqKfWAhVPZ1AKHRKFAhUQ6AEITDAG#v=onepage&q=price%20industrial%20grade%20and%20food%20grade%20salt&f=false> Accessed 17 June 2018.
- E-pao. *Common salt adulteration row: Five students sent to judicial custody*. (2016). <http://e-pao.net/GP.asp?src=8.290516.may16> Accessed 17 June 2018.
- Etymonline (2017). Salary. *On line etymology dictionary*<http://www.etymonline.com/index.php?search=salary> Accessed 17 June 2018.
- EU Parliament. <http://www.europarl.europa.eu/document/activities/cont/201306/20130621ATT68219/20130621ATT68219EN.pdf> Accessed 17 June 2018.
- EUsalt. *Salt production*. (2017). <http://eusalts.com/salt-production> Accessed 17 June 2017.
- Fernández-López, C., Faz Cano, A., Arocena, J. M., & Alcolea, A. (2014). Elemental and mineral composition of salts from selected natural and mine-affected areas in the Poopó and Uru-Uru lakes (Bolivia). *Journal of Great Lakes Research*, 40, 841–850.
- Fitzpatrick, D., Evans-Hurson, R., Fu, Y., Burke, T., Krüse, J., Vos, B., ... Keating, J. J. (2014). Rapid profiling of enteric coated drug delivery spheres via Broadband Acoustic Resonance Dissolution Spectroscopy (BARDS). *Analyst*, 139, 1000–1006.
- Fitzpatrick, D., Evans-Hurson, R., Krüse, J., Vos, B., McSweeney, S., Casaubieilh, P., et al. (2013). The relationship between dissolution, gas oversaturation and outgassing of solutions determined by Broadband Acoustic Resonance Dissolution Spectroscopy (BARDS). *Analyst*, 138, 5005–5010.
- Fitzpatrick, D., Krüse, J., Vos, B., Foley, O., Gleeson, D., O'Gorman, E., & O'Keefe, R. (2012). Principles and applications of Broadband Acoustic Resonance Dissolution Spectroscopy (BARDS): A sound approach for the analysis of compounds. *Analytical Chemistry*, 84, 2202–2210.
- Fitzpatrick, D., Scanlon, E., Krüse, J., Vos, B., Evans-Hurson, R., Fitzpatrick, E., & McSweeney, S. (2012). Blend uniformity analysis of pharmaceutical products by Broadband Acoustic Resonance Dissolution Spectroscopy (BARDS). *International Journal of Pharmaceutics*, 438, 134–139.
- Hyslop, N. P., & White, W. H. (2009). Estimating precision using duplicate measurements. *Journal of the Air & Waste Management Association*, 59, 1032–1039.
- Macias, S. (2014). *Salt – An overview of various types of salts*. Micscape Magazine https://www.microscopy-uk.org.uk/mag/artnov14macro/Macias_AnOverviewOfSalt.pdf (Accessed 17 June 2018).
- Madehow. *Salt*. (2017). <http://www.madehow.com/Volume-2/Salt.html#ixzz4skqPfehE> Accessed 17 June 2018.
- Ministry of Fisheries and Agriculture of Iceland (2012). Clarification regarding salt for human consumption. *Press release from the ministry of fisheries and agriculture of Iceland*. 26 January 2012 http://www.mast.is/english/library/Fr%C3%A9ttatilkynningar/PR_SLRClarificationregardingssalt260112.pdf (Accessed 17 June 2018).
- Newvision. *What's in the salt you use*. (2013). https://www.newvision.co.ug/new_vision/news/1323394/whats-salt Accessed 17 June 2018.
- Penha, F. M., Zago, G. P., Nairyoshi, Y. N., Bernardo, A., & Seckler, M. M. (2018). Simultaneous crystallization of NaCl and KCl from aqueous solution: Elementary phenomena and product characterization. *Crystal Growth & Design*, 18, 1645–1656.
- Satyanarayanan, M., Balaram, V., Gnaneshwar Rao, T., Dasaram, B., Ramesh, S. L., Mathur, R., & Drolia, R. K. (2007). Determination of trace metals in seawater by ICP-MS after preconcentration and matrix separation by dithiocarbamate complexes. *Indian Journal of Marine Sciences*, 36(1), 71–75.
- SDA China. <http://www.sda.gov.cn/WS01/CL0050/168598.html> Accessed 17 June 2018.
- Simon, B. (1981). Dissolution rates of NaCl and KCl in aqueous solution. *Journal of Crystal Growth*, 52, 789–794.
- Snedecor, G. W., & Cochran, W. G. (1980). *Statistical methods* (7th ed.). Ames, USA: The Iowa State University Press.
- Statista. *World salt production from 1975 to 2017 (in million metric tons)*. (2017). <https://www.statista.com/statistics/237162/worldwide-salt-production/> Accessed 17 June 2018.
- Steinhauser, G., Sterba, J. H., Poljanc, K., Bichler, M., & Buchtela, K. (2006). Trace elements in rock salt and their bioavailability estimated from solubility in acid. *Journal of Trace Elements in Medicine and Biology*, 20, 143–153.
- Toboła, T. (2018). Raman spectroscopy of organic, solid and fluid inclusions in the oldest halite of LGOM area (SW Poland). *Spectrochimica Acta Part A: Molecular and Biomolecular Spectroscopy*, 189, 381–392.
- Vos, B., Crowley, S. V., O'Sullivan, J., Evans-Hurson, R., McSweeney, S., Krüse, J., ... Fitzpatrick, D. (2016). New insights into the mechanism of rehydration of milk protein concentrate powders determined by Broadband Acoustic Resonance Dissolution Spectroscopy (BARDS). *Food Hydrocolloids*, 61, 933–945.
- Weseluha-Birczyńska, A., Toboła, T., & Natkaniec-Nowak, L. (2008). Raman spectroscopy of inclusions in blue halites. *Vibrational Spectroscopy*, 48, 302–307.
- Wideopenats. *The 12 different types of salt and how to use each*. (2017). <http://www.wideopenats.com/12-different-types-salt-use/> Accessed 17 June 2018.